4ICEGE Thessaloniki-GREECE 2007

4th International Conference on
Earthquake Geotechnical Engineering
June 25-28, 2007
Paper No. 1590

2–D WAVE EFFECTS IN ALLUVIAL VALLEYS: HOW IMPORTANT AND PREDICTABLE ARE THEY?

Fani Gelagoti [1], George Gazetas[2], Rallis Kourkoulis[1]

ABSTRACT

This paper explores the frequency-dependant characteristics of 2D wave effects in a valley subjected to simple narrow-band excitations with different frequency content. Elastic analyses are initially performed to emphasize on the generated wave-field pattern. The finite elements results reveal the strongly 2-dimensional nature of the problem. Both the distribution pattern and the actual values of the calculated aggravations are controlled by the frequency content of the excitation. It is shown that valley-edges generated surface waves (Rayleigh) and "focusing effects" at the valley sloping boundaries are responsible for the high values of the calculated aggravation. A subsequent set of non-linear analyses is conducted to illustrate the effects of the induced inelasticity on the valley dynamic response. It is shown that when non-linearity is taken into account, the 2-D amplification effects significantly diminish.

Keywords: valley, frequency, aggravation, wavefield pattern, soil-nonlinearity.

INTRODUCTION

Since the work of Trifunac (1973) on the response of a semi-circular canyon subjected to vertical SH-waves, a considerable amount of work on wave scattering phenomena has been reported. In 1979 Sanchez-Sesma & Rosenbluth investigated the ground motion on canyons of arbitrary shape due to incident SH waves, and Bard & Bouchon (1980) studied parametrically the dynamic response of two typical valleys due to incident SH, SV and P waves. They observed that surface waves are generated at the valley boundaries and propagate back and forth resulting in significant amplification. Harmsen & Harding (1981) and Othuki & Harumi (1983) also pointed out that Rayleigh waves are generated at the edges of sediment-filled valleys, when P waves are incident. Of exceptional interest are the simulation of the non-linear response of Marina District during the Loma Prieta earthquake by Zhang & A. S. Papageorgiou (1996) and the work of Bielak et al (1999, 2000) for highly heterogeneous 3-Dimensional structures soil formations.

Experimental studies in the field also provide confirmation (at least in qualitative terms) of the above theoretical work. Particularly, over the last years, fully instrumented test sites have been developed to capture the actual amplification phenomena in sedimentary valleys during earthquake events. Among others the Euroseistest in the Volvi basin in Greece (Chavez-Garcia, 2000, Raptakis, 2000), the Japanese seismograph arrays in Ashigara (Kudo et. Al 1988, 1998) and Ohba valley (Tazoh et al. 1984), the arrays in the alluvial Valley of Parkway in New Zealand (Duggan, 1997) and in Coachella Valley in California (Field et. al. 1992) are some of the best-known.

Despite their obvious significance, 2D wave effects are still not included in most seismic code provisions. Their sensitivity to a plethora of parameters (i.e. geometry, characteristics of input motion, material properties etc) makes them extremely hard to predict. Moreover, as will be seen in this paper soil inelasticity tends to reduce their significance during strong earthquake shaking.

[1] PhD Student, National Technical University, Athens, Greece, Email: fanigelagoti@gmail.com
[2] Professor, School of Civil Engineering, National Technical University, Athens, Greece

GEOMETRY AND GEOTECHNICAL DATA OF OHBA VALLEY

Our case study examines the dynamic response of an extremely–soft alluvial valley near Fujisawa City in Japan (Ohba Valley). The top layers (20-25 meters) consist of extremely soft Holocene alluvium (layers of humus and soft clay) with shear wave velocity (V_S) between 40 to 65 m/s. The underlying substratum consists of Pleistocene diluvia deposits of the Sagami group with V_S around 400 m/s.

Numerical model

A simplified geometry for the Ohba valley and a typical configuration of the numerical model are depicted in Figure 1 (a and b). The soil deposit is assumed homogeneous with V_S = 60 m/s, while the shear wave velocity of the underlying bedrock is 400 m/s. The discretization consists of 1 m x 1m 4-noded quadrilateral elements to ensure the effective representation of the propagating wavelengths for the considered excitation motions. Wave reflections at the base of the formation are avoided by utilizing absorbing boundaries. The lateral boundaries of the model are free to move horizontally not allowing rotation so as to persuasively represent the free-field conditions. The model is subjected to in–plane vertically incident SV waves.

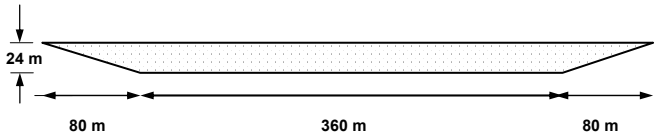

Figure 1a. Simplified Geometry of Ohba Valley

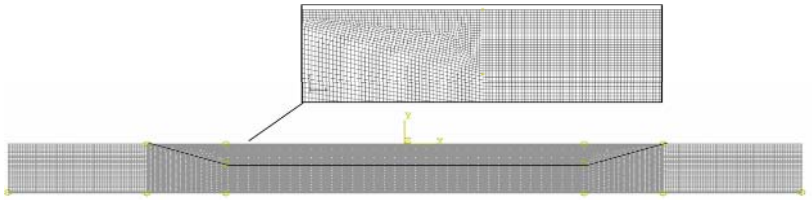

Figure 1b. Configuration of the Finite Element Mesh

2D WAVE EFFECTS SENSITIVE TO EXCITATION FREQUENCY

To investigate the frequency-dependent scattering phenomena, a simple narrow-band Ricker pulse is used for the approximation of the seismic input motion.
Three characteristic problems are examined. The valley is firstly subjected to a Ricker-3 wavelet (high-frequency excitation with characteristic frequency 3 Hz), then to a Ricker-0.5 pulse (long period motion) and finally to a Ricker-1 wavelet (all motions are scaled to 0.3 g). The acceleration time-histories and the corresponding fourier-spectra of the input motions are depicted in Fig 2.
The following trends are worthy of note:
a) For the high frequency excitation Figure 3 depicts the spatial distribution of the aggravation factor, defined as the ratio between the peak ground accelerations in the 2D and 1D analysis. The analysis is elastic with low damping ratio equal to 2%. The following trends are observed**:**
In the central part of the valley 1D soil amplification is the prevailing phenomenon while strongly 2-D phenomena are localized at the valley corners (the local peak value reaches 2.5!) It is believed that the trapping of obliquely transmitted body waves amplifies the experienced motion near the edges resulting in significant aggravations (“focusing effects”). The particular aggravation pattern is reminiscent of actual earthquake damage distributions. In Caracas, for example, the high concentration of damage in the area of Palos Grandes during the 1967 earthquake was attributed to the steep slope of the supporting bedrock at the northern boundary of the 3 km long sendimentary valley.

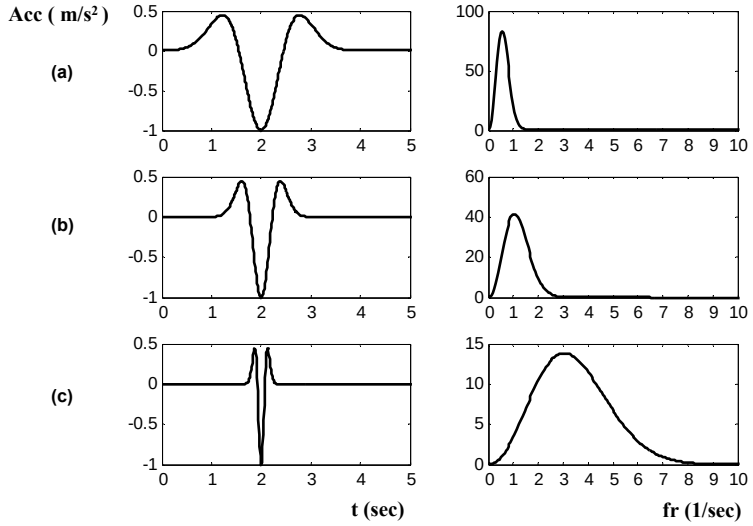

Figure 2. Acceleration time-histories (left column)and corresponding fourier spectra (right column) of (a) a ricker-0.5 wavelet (upper), (b) a ricker-1 wavelet (middle) and (c) a ricker-3 wavelet (bottom)

To detect the generated waveforms a useful numerical "diagnostic" tool is the seismogram synthetics. Fig 3 depicts the synthetic of the horizontal acceleration. The following waveforms are clearly distinguished:

1. *incident SV waves (C = V_s)*
2. *Refracted inclined body waves* by the wedge-shaped boundary of the valley (denoted as c_a)
3. *Rayleigh waves* generated at the valley edges and propagating horizontally along the surface in opposite directions (C = R_i).

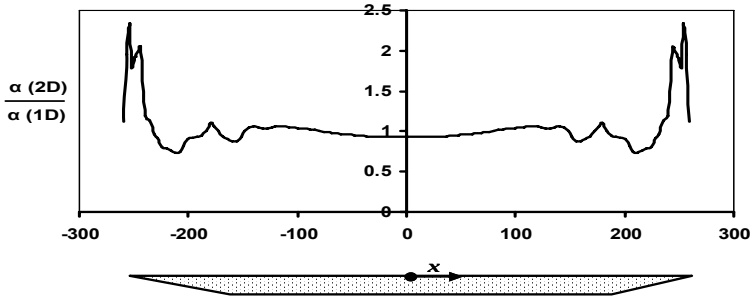

Figure 3. Aggravation of peak ground acceleration along the surface (Ricker-3, ξ = 2%).

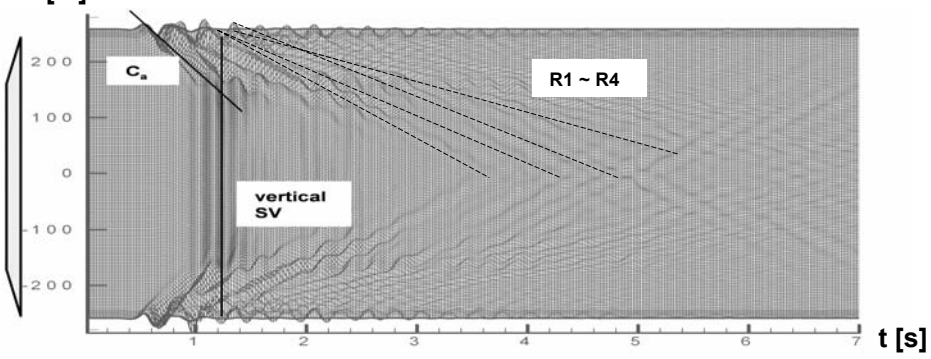

Figure 4. Seismogram synthetics of horizontal motion along the valley Ricker-3, ξ = 2%)

b) For low frequency excitation (input motion Ricker-0.5), the spatial distribution of the aggravation factor is depicted in Fig 5. Here the pattern is completely reversed:

It is clear that the basin-induced waves strongly "contaminate" the 1D valley response. The calculated aggravations at the central region of the valley are high (reach the value of 1.7), whereas toward the edges the aggravation factor drops to 1 (implying no 2D amplification). Particularly, the peak aggravation in the middle of the valley is the result of the constructive interference of Rayleigh waves. The symmetrical shape of the valley undoubtedly plays a significant role, as the surface waves reach the middle in phase. Therefore, potential imperfections in the valley geometry may completely modify this idealized picture of the calculated aggravations. The observed local maxima around x = $\pm$ 130 m are attributed to the superposition of vertically propagating SV waves with horizontally propagating Rayleigh waves. On the other hand, the complete absence of "focusing" phenomena above the oblique boundaries of the valley can be explained given the wavelengths of the incident body waves ($\lambda = V_s/f$ = 60 / 0.75 = 80 m: significantly bigger than the typical dimension of the bedrock irregularity).

Figure 6 depicts the seismograph synthetic of the horizontal acceleration. The figure is self-explanatory; the basin-induced Rayleigh waves that travel towards the valley centre are vividly observed.

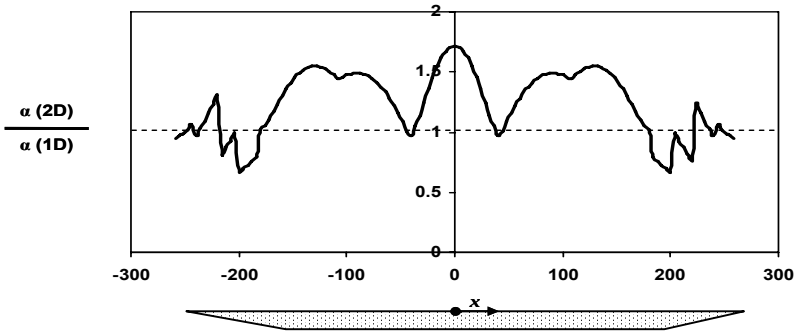

Figure 5. Aggravation of peak ground acceleration along the surface (Ricker-0.5 ξ = 2%).

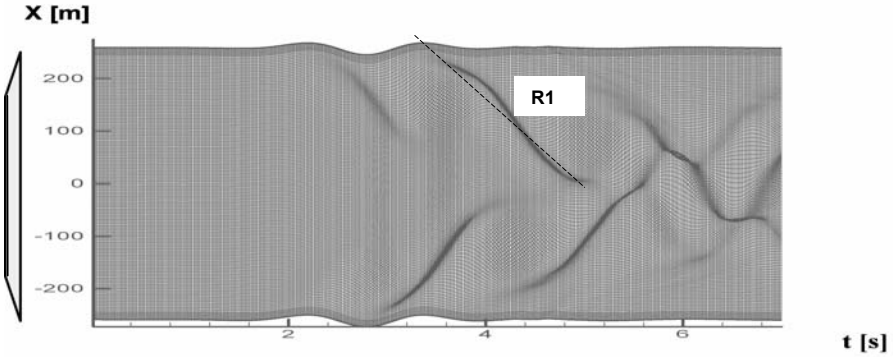

Figure 6. Seismogram synthetics of horizontal motion along the valley (Ricker-0.5, ξ = 2%)

c) For intermediate-frequency excitation a Ricker-1 pulse is imposed. The computed aggravation pattern is illustrated in Fig 7. Again in this case the 2D nature of the response is dominant (aggravation reaches the value of 1.6 at several points along the valley). Interestingly the aggravation pattern in this case looks like a composition of the two previously examined "extreme" frequencies (Ricker-0.5 and Ricker-3 excitation). Strongly 2D phenomena are displayed both near the valley edges, due to the multiply reflected waveforms at the sloping bedrock, and at the central part of the valley due to the laterally propagating surface waves. Note also the strong fluctuations in the value of aggravation between neighboring locations.

The resulting wavefield pattern is schematically illustrated in the seismogram synthetics of Fig 8. All the different waveforms are clearly depicted: body waves (SV), diffracted waves (C_a) and two modes of Rayleigh waves (R_1 and R_2 respectively).

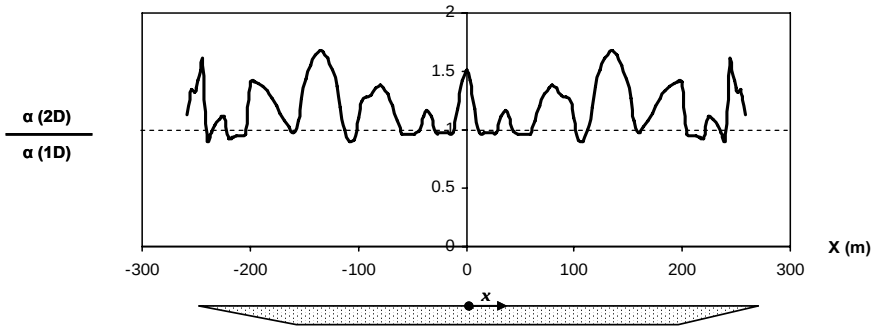

Figure 7. Aggravation of peak ground acceleration along the surface (Ricker-1 ξ = 2%).

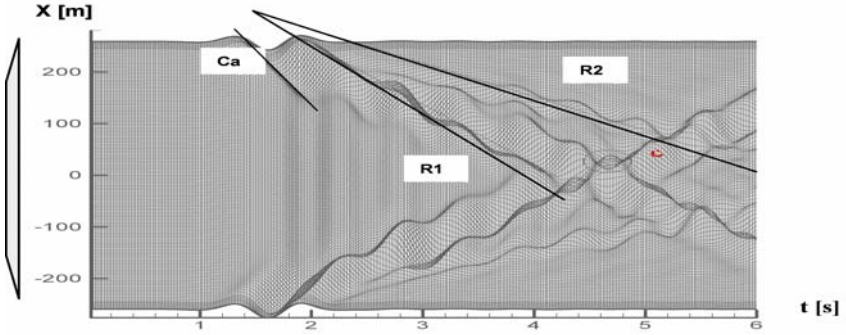

Figure 8. Seismogram synthetics of horizontal motion along the valley (Ricker-1, ξ = 2%)

EFFECTS OF SOIL NON-LINEARITY

In the preceding the dynamic response of the valley was considered elastic (with small damping). However, the "reality" is neither elastic nor linear. At low strain amplitudes, the soil stiffness is high, but decreases with increasing strain. At the same time the damping ratio increases with increasing strain amplitude. The scope of this paragraph is to reveal whether and to what extent the nonlinear soil behavior affects the dynamic valley response. Initially, the simplified case of an elastic soil with increasing levels of viscous damping is investigated while the results of a non-linear analysis are presented in the ensuing.

Role of damping on the 2D-response of the Valley

The valley is subjected to a Ricker-3, a Ricker-0.5 and a Ricker-1 wavelet, and its response is investigated for levels of damping between 2% and 10%. Again all input motions are scaled at 0.3 g. Figure 8 portrays the spatial distribution of the aggravation factor along the ground surface for the examined motions and for damping ratio 2%, 5%, 7.5% and 10% respectively. It is observed that increasing damping mainly affects the generated surface waves. The local maxima at the central part of the valley attributed to Rayleigh wave interferences are dramatically affected. Moving towards the edges however, the effect of increasing damping becomes less pronounced. This implies that the aggravation peaks caused by multiple wave reflections on the oblique boundaries are only slightly reduced.

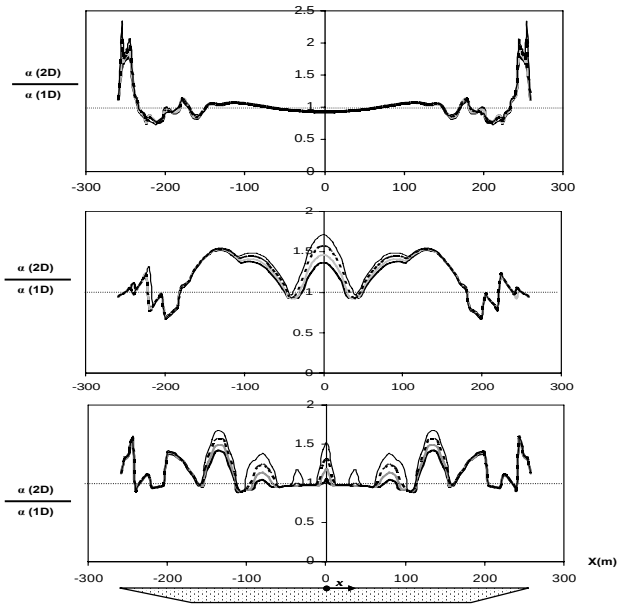

Figure 8. Aggravation of p.g.a. along the surface (valley subjected to a Ricker-3, a Ricker- 0.5 and a Ricker-1 wavelet) and for damping ratios equal to 10% (black), 7.5% (gray), 5% (dotted line), and 2% (thin black line)

Non-linear Response

The non-linear analyses are conducted with the numerical algorithm QUAD4M by assuming equivalent linear soil behavior. (Soil non-linearity is taken into account approximately by an iterative procedure, according to which the values of soil stiffness and damping depend on the level of shear strain). Again the discretization consists of 1 m x 1m 4-noded quadrilateral elements. It is believed that this mesh can realistically ensure the effective representation of the propagating wavelengths at least for excitation frequencies up to 5 Hz. The G–γ and ξ–γ curves that we used in our analyses are the experimental curves for plasticity index PI=50 (Dobry and Vucetic, 1991). Two extreme cases are examined. The valley is subjected to a Ricker-3 and a Ricker-0.5 wavelet both scaled at 0.3 g.

Figures 9 and 10 present the spatial distribution of the aggravation factor along the valley surface for both the linear and the non-linear case, when the model is subjected to a Ricker-3 and a Ricker-0.5 pulse respectively. The following are observed:
(a) In the case of the high-frequency excitation (Ricker-3), the overall trends are retained, but the amplitude of the aggravation is considerably reduced; the peak values drop from 2.5 to 1.5 (Fig 9). The average peak strain level reached is 15 %.
(b) On the other hand, when the input motion is the long period Ricker-0.5 the induced non-linearity completely modifies the aggravation pattern. No maxima exist at the central part of the valley. However, near the valley edges significant peaks that were not observed in the elastic case have now emerged (Figure 10). In this case the average peak strain level reached is 59 %.

In Figure 11 the seismogram synthetic for the inelastic problem, when the excitation is Ricker-0.5, is illustrated. The corresponding synthetic for the high-frequency excitation (Ricker-3) is depicted in Figure 12. Note that in this case the signal on the very edges looks strange because the duration and the number of cycles is larger than for the simple Ricker wavelet. It is believed that for the particular case the mesh is not small enough to accurately represent the very high frequencies (> 5 Hz) given the reduced velocity values. However this numerical edge effect doesn't affect the qualitative conclusions derived. It is observed that regardless the frequency content of the excitation motion the increased level of non-linearity strongly attenuates the basin-generated surface waves. Note also the significant drop in their propagation velocity.

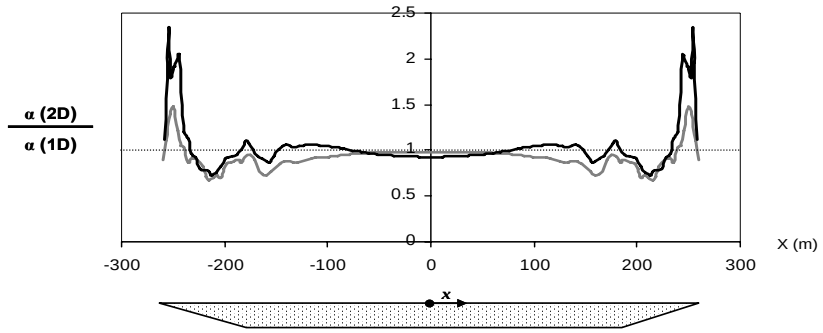

Figure 9. Aggravation of p.g.a. when the valley is subjected to a Ricker-3 wavelet for elastic (black line) and non-linear (gray line) soil.

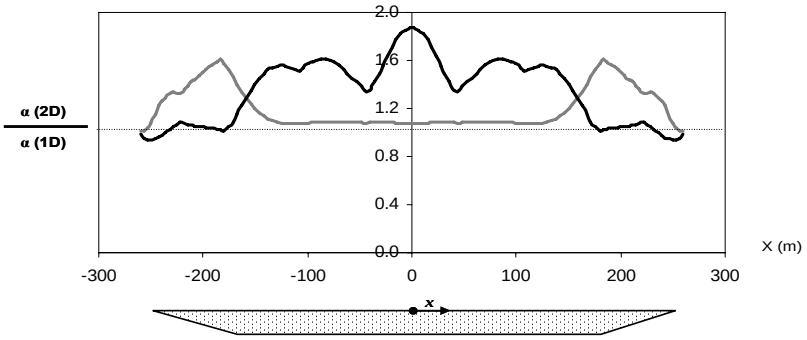

Figure 10. Aggravation of p.g.a. when the valley is subjected to a Ricker-0.5 wavelet for elastic (black line) and non-linear (gray line) soil.

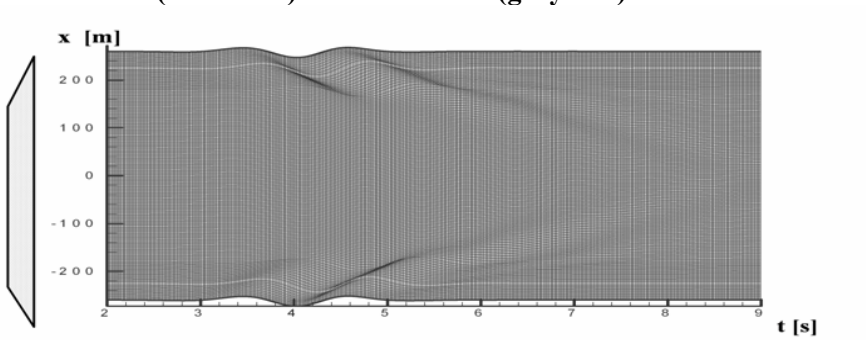

Figure 11. Seismogram synthetics of the horizontal motion along the valley when the soil is assumed non-linear and the excitation motion is a Ricker-0.5

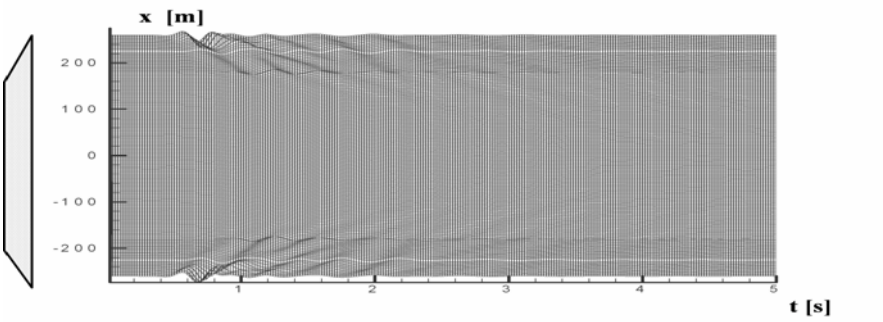

Figure 12. Seismogram synthetics of the horizontal motion along the valley when the soil is assumed non-linear and the excitation motion is a Ricker-3

CONCLUSIONS

1. In the elastic problems the dynamic response of the valley is strongly 2-Dimensional. 1-dimensional analysis is inadequate to predict the calculated ground motions.
2. Valley induced surface waves (Rayleigh) and "focusing effects" at the valley edges are responsible for the high values of the calculated aggravation.
3. When the inelastic soil-behaviour is taken into account the trends are reversed: The wavefield pattern is dominated by propagating body waves, and the 1-D amplification theory in general terms can satisfactorily reproduce the surface ground motion. The only exception is the highly 2-D response near the valley edges caused by the multiply reflected body waves on the inclined boundaries.

REFERENCES

Dominic Assimaki, George Gazetas, and Eduardo Kausel.(2005). Effects of Local Soil Conditions on the Topographic Aggravation of Seismic Motion: Parametric Investigation and Recorded Field Evidence from the 1999 Athens Earthquake, *Bull. Seism. Soc. Am.*95, 1059-1089

Bard P. Y. and M. Bouchon. (1980a). The seismic response of sediment-filled valleys. Part I. The case of incident *SH* waves, *Bull. Seism. Soc. Am.* 70, 1263-1286

Bard P. Y. and M. Bouchon (1980b). The seismic response of sediment-filled valleys. Part II. The case of incident *P* and *SV* waves, *Bull. Seism. Soc. Am.* 70, 1921-1941

Bielak J., Xu J., & O. Ghattas. (1999). Earthquake Ground motion and Structural Response in alluvial Valleys, *Journal of Geotechnical and Geoenviromental Engineering.*

Bielak J., Hisada Y., Bao H., Xu J. & Gatas O. (2000). One- vs two- or three-dimentional effects in sendimentary valleys. *Proccedings of the 12th World Conference on Earthquake Engineering, New Zealand.*

Chávez-García F. J., Stephenson W. R., and M. Rodriguez.(1999). Lateral propagation effects observed at Parkway, New Zealand: a case history to compare 1D versus 2D site effects, *Bull. Seism. Soc. Am.* 89,718 -732.

Chavez-Garcia F., Raptakis D.G., Makra K.A. and, K.D. Pitilakis. (2000). Site Effects at Euroseistest-II. Results from 2D Numerical Modeling and Comparison with Observations. *Soil Dyn. Earth. Eng*. 19 (1), 23-39.

Duggan E. B. (1997). Shallow seismic structure of Parkway Basin, Wainuiomata, New Zealand. *B.Sc. (Hons) thesis* , Victoria University of Wellington, New Zealand.

Field, E. H., Jacob K. H., Barstow N., and P. A. Friberg.(1992). Coachella Valley site-response experiment using Landers earthquake aftershocks in southern California, *Bull. Natl. Center Earthquake Eng. Res. 6, 8-11.*

Harmsen S. C. and S. T. Harding (1981). Surface motion over a sedimentary valley for incident plane *P* and *SV* waves, *Bull. Seism. Soc. Am.* 71, 655-670

Kudo K., E. Shima E., and M. Sakaue. (1988). Digital strong motion accelerograph array in Ashigara valley, *Proc. 9th World Conf. Earthquake Eng., Tokyo, Japan* ,119 -124.

Kudo K. and Y. Sawada. (1998). A brief review on the Ashigara Valley blind prediction test and some follow-up studies, *The Effects of Surface Geology on Seismic Motion*, 305-312.

Ohtsuki, A., and K. Harumi. (1983). Effect of topography and subsurface inhomogeneities on seismic SV waves, *Earthquake Eng. Struct. Dyn.* 11,441-462.

Proctor R. J. (1968). Geology of the Desert Hot Springs-Upper Coachella Valley area, California, *Calif. Div. Mines Geol., Spec. Rept. 94,* 50.

Raptakis D.G., Chavez-Garcia F., Makra K.A., and K.D. Pitilakis. (2000). Site Effects at Euroseistest-I. 2D Determination of the Valley Structure and Confrontation of the Observations with 1D Analysis. *Soil Dyn. and Earth. Eng.*.19 (1), 1-22

Sanchez-Sesma F. J. and E. Rosenbluth (1979). Ground motion at canyons of arbitrary shape under incident SH waves. *Intern. J. Earthquake Eng. Struct. Dyn.* 7, 441-450

Tazoh T., Dewa K., Shimizu K., & Shimada M. (1984). Observations of earthquake response behavior of foundation piles for road bridge. *Proceedings of the 8th World Conference on Earthquake Enginnering, 3, 577-584.*
Trifunac M. D. (1973). Scattering of plane *SH* waves by a semi-cylindrical canyon, *Intern. J. Earthquake Eng. and Dyn. of Struct.* 1, 267-281.
Zhang B. and A. S. Papageorgiou. (1996). Simulation of the response of the Marina District Basin, San Francisco, California, to the 1989 Loma Prieta earthquake, *Bull. Seism. Soc. Am.* 86, 1382-1400